JOURNAL OF SOLID STATE CHEMISTRY **139,** 22–26 (1998)
ARTICLE NO. SC987783

Toward Pillared Metal Sulfides: Encapsulation and Rietveld Structural Characterization of the $Al_{13}O_4(OH)_{24}(H_2O)_{12}^{7+}$ Cluster into MoS_2 and WS_2

Joy Heising, François Bonhomme, and Mercouri G. Kanatzidis[1]

Department of Chemistry and Center for Fundamental Materials Research, Michigan State University, East Lansing, Michigan 48824

Received May 12, 1997; in revised form February 3, 1998; accepted February 6, 1998

The synthesis of $[Al_{13}O_4(OH)_{24}(H_2O)_{12}]_xMS_2$ ($x = 0.02$–0.05, $M = Mo$; $x = 0.02$–0.055, $M = W$) was accomplished by a precipitative encapsulation technique using single layers of MS_2. The products were characterized by powder X-ray diffraction, energy dispersive spectroscopy (EDS), thermal gravimetric analysis (TGA), ^{27}Al MAS-NMR, room temperature electrical conductivity measurements, and surface area measurements. Powder X-ray diffraction patterns show an expansion of approximately 9.9 Å. ^{27}Al MAS-NMR indicates that the cluster is intact between the MS_2 layers. One-dimensional electron density mapping and Rietveld refinement performed on the powder diffraction data show that the cluster is oriented with its C_3 symmetry axis perpendicular to the layers. The samples exhibit conductivity values from 3 to 14 S/cm. TGA shows that the cluster is completely stable to 100°C, and largely stable to 330°C. Surface area measurements suggest that the space between the clusters is not accessible.

Since Barrer and MacLeod reported the first pillared species in 1955 (1), much effort has gone into the development of microporous materials for use as size-selective molecular sieves and catalysts. Zeolites and pillared clays have been studied extensively for these applications (2, 3); however, these materials are insulators. Because WS_2 and MoS_2 have interesting electronic and optical properties, pillared WS_2 and MoS_2 may be useful for unique applications similar to but distinct from the applications for zeolites and pillared clays. The availability and relatively low cost of MoS_2 make it an especially desirable chalcogenide host.

The practical applications of MoS_2 itself are quite diverse. These include use as a solid lubricant (4), a catalyst (5), and a host material for solid state batteries (6). MoS_2 has been intercalated with a variety of compounds, including polymers (7, 8), small organic molecules (9), and inorganic complexes such as ferrocene (10) and the cobalt clusters $Co_6Q_8(PR_3)_6$ (Q = S, Se, Te; R = alkyl) (11). WS_2 is isostructural to MoS_2, with similar intercalation chemistry, although less well explored (12).

Despite the considerable intercalation history of layered dichalcogenides, microporous pillared chalcogenides have not been reported to date. The intercalation of TaS_2 with $Al_{13}O_4(OH)_{24}(H_2O)_{12}^{7+}$ and the iron cluster $Fe_6S_8(PEt_3)_6^{2+}$ has been achieved, but no information about the porosity of these materials is reported (13). Intercalation of the $Co_6Q_8(PR_3)_6$ clusters into MoS_2 increase the surface area three- or fourfold, but TEM studies show that the lamellar expansion due to the clusters is localized (14). We have chosen to explore $Al_{13}O_4(OH)_{24}(H_2O)_{12}^{7+}$ as a pillaring agent for MoS_2 because of its successful history as a pillaring agent for clays (3, 15), and because alumina-supported MoS_2 is used as a catalyst for hydrodesulfurization (5).

The preparation of the samples was conducted as follows: $LiMS_2$ (M = Mo, W) (16) was exfoliated (17) in deionized, deoxygenated H_2O via a redox reaction, generating single layers, lithium hydroxide, and hydrogen gas:

$$LiMS_2\ (s) + H_2O\ (l) \rightarrow MS_{2(\text{single layers})} + LiOH(aq) + 0.5H_2\ (g) \quad [1]$$

Eq. [1] has been proposed for the exfoliation of MS_2 by Divigalpitiya *et al.* (9). The exfoliated suspension was centrifuged and rinsed three times in order to reduce the pH of the solution to about 7, then resuspended in H_2O. This suspension was added to various amounts of an (approximately) 0.03 M solution of $[Al_{13}O_4(OH)_{24}(H_2O)_{12}]Cl_7$ in H_2O (18). After stirring for several hours the product was isolated via centrifuge, rinsed, and dried on a glass slide (19). The product was a shiny film which could be scraped off the glass and ground to a fine black powder.

The predominance of the 00l reflections in the X-ray powder diffraction pattern indicates that the layers are well oriented, with a typical expansion of about 9.9 Å (see Fig. 1).

[1]To whom correspondence should be addressed.

0022-4596/98 $25.00

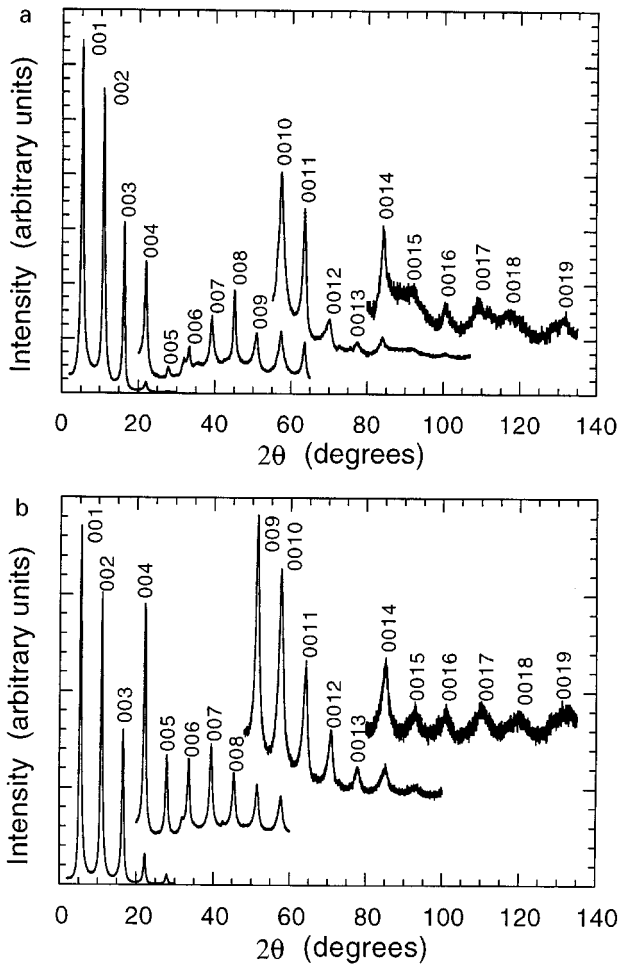

FIG. 1. X-ray diffraction patterns of (a) $[Al_{13}O_4(OH)_{24}(H_2O)_{12}]_{0.05}MoS_2$ and (b) $[Al_{13}O_4(OH)_{24}(H_2O)_{12}]_{0.055}WS_2$ used for electron density maps and Rietveld refinements. Strong preferential orientation of the samples leads to the observation of only the 00*l* reflections.

This value is consistent with the dimensions of the cluster, which are about 10.2 Å along the C_3 symmetry axis, 11.5 Å along one C_2 symmetry axis, and 12.8 Å along the other C_2 axis (average diameter 11.5 Å) (see orientations A, B, and C, respectively, in Fig. 2). Our observed expansion suggests that the cluster is oriented with its C_3 axis perpendicular to the layers.

After conversion to the oxide (31), loadings of the cluster were calculated using energy dispersive spectroscopy (EDS) to quantitate an Al : Mo ratio. The observed values ranged from $[Al_{13}O_4(OH)_{24}(H_2O)_{12}^{7+}]_{0.02}MoS_2$ to $[Al_{13}O_4(OH)_{24}(H_2O)_{12}^{7+}]_{0.05}MoS_2$. The theoretical maximum loading of the cluster (if one assumes hcp packing of the spheres) is $[Al_{13}O_4(OH)_{24}(H_2O)_{12}^{7+}]_{0.06}MoS_2$. Conversion to oxide was not necessary for samples containing WS_2, and comparable stoichiometries (up to $[Al_{13}O_4(OH)_{24}(H_2O)_{12}^{7+}]_{0.055}WS_2$) were observed by EDS.

Lithiated and exfoliated MoS_2 was presumed to be neutral because it is possible to intercalate neutral molecules (9). One surprising discovery was that no chloride is detected in the samples by EDS. It appears that this cation intercalates without its chloride anion. The strong intensity of reflections, the relatively high degree of order, and the ease of encapsulation of the cation seem to indicate that the MoS_2 and WS_2 have some negative charge. This would explain the driving force for the intercalation. We have observed intercalation of other cations without anions, consistent with a negative charge on the layers (21). The observed loadings of the cluster, presuming no change in its charge, suggest that the negative charge on the layers is between 0.1 and 0.4. This wide range of possible negative charge suggests that the charge on the aluminum cluster may vary, depending on the loading. Studies to probe the ionicity of the layers in detail are in progress.

In order to probe the structure and orientation of the encapsulated cluster, one-dimensional electron density mapping calculations were carried out on samples of the cluster in MoS_2 and WS_2, prepared using excess cluster to generate particularly well-ordered materials (22). The electron density maps were obtained using the equation [2]

$$\rho(z) = (1/c)[2\sum F_l \cos(2\pi lz)], \qquad [2]$$

where c is the c-axis, F is the structure factor, and $z = -0.2$–1.2 in increments of 0.01. Sixteen 00*l* reflections were used in the calculations for the sample containing MoS_2 and eighteen 00*l* reflections for the sample containing WS_2. Comparison of the observed data to theoretical data for the intercalated cluster in three possible orientations (depicted in Fig. 2) for both samples supported the initial supposition that the cluster is oriented with its C_3 axis oriented perpendicular to the layers in both hosts (see Fig. 3). This orientation has been observed in clays with an expansion of 9.6 Å (23). In this orientation, qualitatively one would expect to see four peaks for the four planes containing oxygen atoms interspersed with three, somewhat weaker peaks corresponding to the less densely occupied aluminum-containing planes. The electron density map calculated from the diffraction data for MoS_2 (Fig. 3a, pattern O) matches the calculated pattern for orientation A in Fig. 2 (Fig. 3a, pattern A) in shape and location of peaks, although two peaks from the aluminum planes seem enhanced and two of the oxygen planes seem weak in the experimental pattern. Both the locations and intensities of the peaks for orientations B and C do not match the pattern calculated from the diffraction data. The data from the cluster in WS_2 also matches orientation A, but in this case both the patterns from the diffraction data (O) and for the theoretical pattern (A) have somewhat asymmetric peaks for two of the oxygen planes (Fig. 3b). The peaks for the sulfur atoms are split due to a combination of a dynamic range problem between the

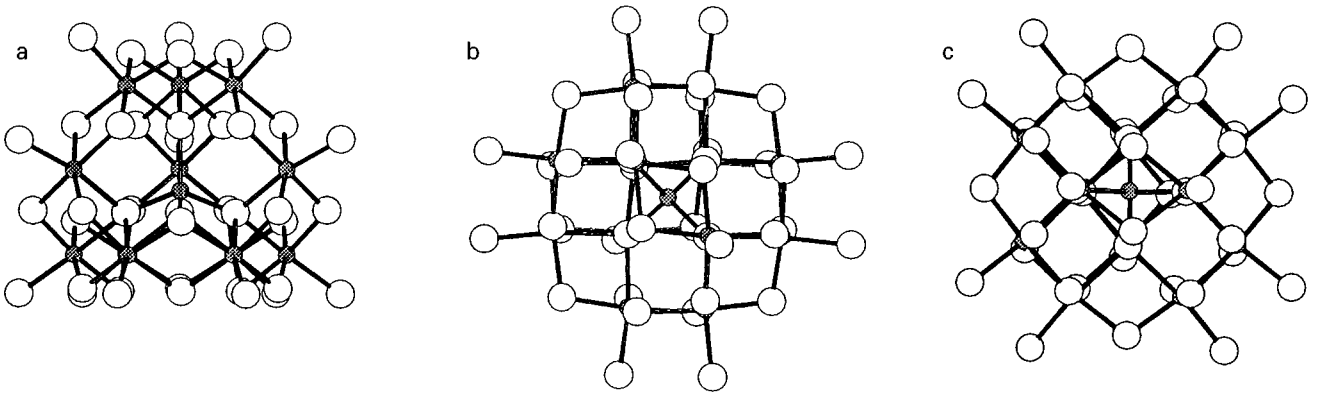

FIG. 2. Three possible orientations of the cluster between the layers.

heavy tungsten and lighter sulfur (i.e., the very strong atomic scattering factor of W), and a Fourier truncation caused by the use of a finite number of reflections.

In order to confirm the cluster orientation found from the analysis of the electron density maps, a Rietveld refinement of the three structural models was carried out using the program FULLPROF (24) on the powder X-ray diffraction data from intercalated WS_2. The cautious application of the Rietveld method, which uses the raw experimental diffractogram and does not require extensive and error-prone data treatment, seems to be a straightforward and efficient way to discriminate among various models of cluster orientation. It is not subject to some of the problems of electron density mapping, such as series termination errors and lack of resolution due to an insufficient number diffraction peaks. Furthermore, it is possible to exclude the first diffraction peaks, which are most affected by systematic errors in the geometrical factor because of the high degree of preferred

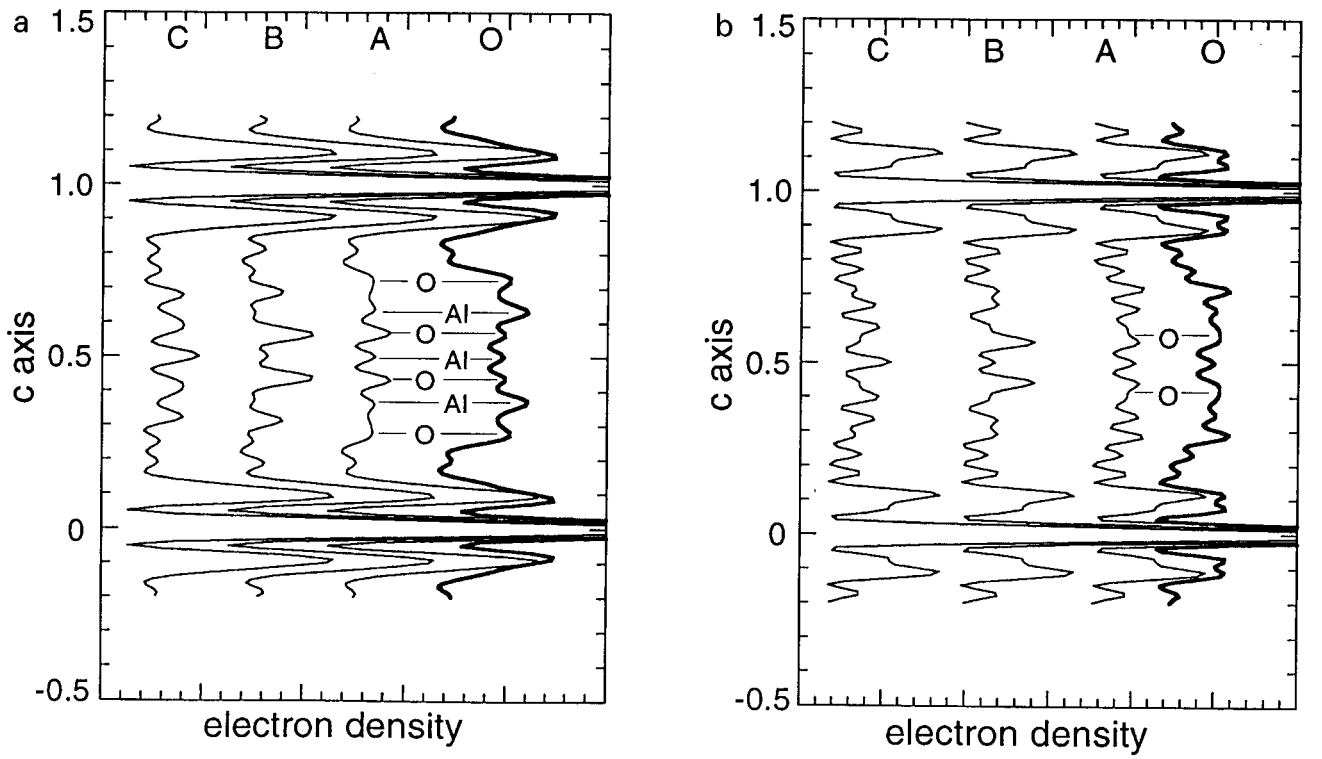

FIG. 3. One-dimensional electron density maps of (a) $[Al_{13}O_4(OH)_{24}(H_2O)_{12}]_{0.05}MoS_2$ and (b) $[Al_{13}O_4(OH)_{24}(H_2O)_{12}]_{0.055}WS_2$. The patterns labeled (O) were generated from the diffraction data. The remaining patterns were calculated from three possible orientations of the cluster depicted in Fig. 2. Orientation (A) matches best with the experimental data for both samples.

orientation. In electron density calculations, the absence of those peaks could preclude the interpretation of the resulting map (25). The experimental data were fit with the Pearson VII peak profile function, and a model for the asymmetry of the peaks was included (26). Sixteen 00*l* reflections were used, falling within the range $13.5^\circ \leq 2\theta \leq 125^\circ$, with a step size of 0.16°. Owing to the small number of Bragg peaks in the diffraction pattern, the number of free structural parameters was kept to a minimum (27). The results of the refinements are summarized in Table 1. The WS_2 column corresponds to a model without cluster. Orientation B, giving worse results than the WS_2 host alone, is clearly to be rejected. Orientation A, which was favored by the electron density maps, gives better results than orientation C. There is almost certainly water between the layers as well; however, while including ordered water in the models improves the correlation between the theoretical and experimental patterns, it does not change the relative ranking of the models. A larger *d* spacing (11 Å) and electron density mapping calculations indicate that the cluster has a different orientation (B in Fig. 2) in MoO_3 (30).

Thermal gravimetric analysis under nitrogen shows continuous gradual weight loss with an inflection point around 300°C. Powder X-ray diffraction indicates that the cluster is intact after heating to 120°C. After heating to 280°C and 330°C the cluster is still present in the sample, but the material does not diffract as well and a "restacked" peak at 6.1 Å begins to appear. On heating the sample to 650°C the cluster degrades and the layers collapse, resulting in a material with a *d*-spacing only slightly larger than the restacked, unintercalated material. For $[Al_{13}O_4(OH)_{24}(H_2O)_{12}]_{0.04}MoS_2$, there are about 0.72 water molecules per molybdenum (about 20 per aluminum cluster) (32).

TABLE 1
Summary of the Rietveld Powder Refinement on $[Al_{13}O_4(OH)_{24}(H_2O)_{12}]_{0.055}WS_2$

	WS_2	Orientation A	Orientation B	Orientation C
R_{wp}	12.0%	7.8%	13.6%	9.4%
χ^2	29.1	12.9	37.6	17.7
R_I	13.6	5.8	16.1	7.3
d_{DW}	0.170	0.391	0.135	0.271
z_S	0.095(3)	0.096(1)	0.094(3)	0.096(1)
$\Delta z_{cluster}$	—	0.010(6)	0.005(5)	0.031(7)

Note. R_{wp} is the weighted agreement factor based on the observations, χ^2 is the goodness of fit, R_I is the agreement indices based on "observed" integrated intensities, and d_{DW} is the value of the Durbin-Watson statistic (28), an indicator of the degree of correlation among the residuals. $\Delta z_{cluster}$ is the displacement of the center of the cluster from its original position at $z = 1/2$. The standard deviations given by the refinement program are typically underestimated and they were multiplied by a scale factor in order to make them more realistic (29).

Surface area measurements of the samples were conducted; all exhibited low surface areas (e.g., 9.4 m^2/g) relative to restacked MoS_2 (10 m^2/g). Drying in a vacuum overnight over P_2O_5, soaking in ethanol and critical point drying in CO_2, and heating to 100°C, 120°C, or 300°C in flowing nitrogen or vacuum did not improve the surface areas of the samples. For one sample heated to 120°C, the vacuum in the outgassing apparatus even reached $\sim 10^{-5}$ torr, and powder X-ray diffraction after the measurements showed little change in the *d*-spacing, but the surface area was no better than restacked MoS_2. Given that there is sufficient space between the clusters to accommodate intercalated water molecules, even in the most fully loaded samples that have been observed, it is surprising that the surface area values of the materials are not better than restacked MoS_2. This finding indicates that the volume vacated by the departing water molecules becomes inaccessible to the nitrogen molecules (34).

The electrical conductivity of thin films of the materials, dried on glass microscope slides, was measured. If measured within 24 h of the exfoliation, the conductivity of the cluster intercalated MoS_2 ranges from 3–14 S/cm. The metallic properties of these samples can be attributed to a phase transition in MoS_2 on lithiation (33).

MAS-NMR ^{27}Al spectra of several samples with various loadings of cluster exhibited a peak at about 64 ppm corresponding to the tetrahedral aluminum at the center of the cluster. This peak has been observed by others who have intercalated the cation into various hosts and is found in the sulfate salt of the unintercalated cluster (10, 15). The spectra also exhibit a broad peak centered around 0 ppm which can be attributed to octahedral aluminum.

In conclusion, we have seen through X-ray diffraction, MAS-NMR, and EDS that $Al_{13}O_4(OH)_{24}(H_2O)_{12}^{7+}$ intercalates into MoS_2 and WS_2. The cation appears to intercalate without its anion, suggesting a negative charge on the layers. Electron density mapping and Rietveld powder refinement show that the cluster maintains its structural integrity while encapsulated and is oriented with its C_3 symmetry axis perpendicular to the layers. The materials are conductive and thermally stable up to 280°C. Applications for this material will be explored.

ACKNOWLEDGMENTS

Financial support from the National Science Foundation CHE 96-33798, (Chemistry Research Group) is gratefully acknowledged. This work made use of the SEM facilities of the Center for Electron Optics at Michigan State University. We thank Professor Thomas J. Pinnavaia for fruitful discussions and help with the BET surface area measurements.

REFERENCES

1. R. M. Barrer and D. M. MacLeod, *Trans. Faraday Soc.* **51,** 1290 (1955).

2. R. M. Barrer, "Zeolites and Clay Minerals as Sorbents and Molecular Sieves," p. 407. Academic Press, New York, 1978.
3. (a) T. J. Pinnavaia, "Characterization of Catalytic Materials," (I.E. Wachs, Ed.), p. 149. Manning Publications Co., Greenwich CT, 1992; (b) I. D. Johnson, T. A. Werpy, and T. J. Pinnavaia, *J. Am. Chem. Soc.* **110,** 8545 (1988).
4. P. D. Fleischauer, *Thin Solid Films* **154,** 309 (1987).
5. (a) S. Harris and R. R. Chianelli, *J. Catalysis* **86,** 400 (1984); (b) O. Weisser and S. Landa, "Sulfided Catalysts, Their Properties and Applications." Pergamon, New York, 1973; (c) R. Prins, H. J. De Beer, and G. A. Smorjai, *Catal. Rev.—Sci. Eng.* **32,** 1 (1989).
6. (a) C. Julien, S. I. Saikh, and G. A. Nazri, *Mater. Sci. Eng.* **B15,** 73 (1992); (b) H. Tributsch, *Faraday Discuss. Chem. Soc.* **70,** 190 (1980).
7. (a) R. Bissessur, M. G. Kanatzidis, J. L. Schindler, and C. R. Kannewurf, *J. Chem. Soc., Chem. Commun.* 1582 (1993); (b) M. G. Kanatzidis, R. Bissessur, D. C. De Groot, J. L. Schindler, and C. R. Kannewurf, *Chem. Mater.* **5,** 595 (1993); (c) L. Wang, J. L. Schindler, J. A. Thomas, C. R. Kannewurf, and M. G. Kanatzidis, *Chem. Mater.* **7,** 1753 (1995).
8. J. P. Lemmon and M. M. Lerner, *Chem. Mater.* **6,** 207 (1994).
9. (a) W. M. R. Divigalpitiya, R. F. Frindt, and S. R. Morrison, *Science* **246,** 371 (1989); (b) W. M. R. Divigalpitiya, R. F. Frindt, and S. R. Morrison, *J. Mater. Res.* **6,** 1103 (1991).
10. H. Tigaya, T. Hashmoto, M. Karasu, T. Izumi, and K. Chiba, *Chem. Lett.* 2113 (1991).
11. R. Bissessur, J. Heising, W. Hirpo, and M. G. Kanatzidis, *Chem. Mater.* **8,** 318 (1996).
12. (a) W. Rudorff, *Chimia* **19,** 489 (1965); (b) E. Bayer and W. Rudorff, *Z. Naturforsch., B* **27,** 1336 (1972); (c) R. Schöllhorn, J. Bethel, and W. Paulus, *Rev. Chim. Miner.* **21,** 545 (1984); (d) B. K. Miremadi and S.R. Morrison, *J. Appl. Phys.* **63,** 4970 (1988).
13. (a) A. Lerf, E. Lalik, W. Kolodziejski, and J. Klinowski, *J. Phys. Chem.* **96,** 7389 (1992); (b) L. F. Nazar and A. J. Jacobson, *J. Chem. Soc., Chem. Commun.* 570 (1986); (c) L. F. Nazar and A. J. Jacobson, *J. Mater. Chem.* **4,** 149 (1994).
14. J. Brenner, C. Marshall, L. Ellis, N. Tomczyk, J. Heising, R. Bissessur, and M. G. Kanatzidis, work in progress.
15. D. Plee, F. Borg, L. Gatinau, and J. J. Fripiat, *J. Am. Chem. Soc.* **107,** 2362 (1985).
16. (a) D. W. Murphy, F. J. DiSalvo, G. W. Hull Jr., and J. V. Wasczak, *Inorg. Chem.* **15,** 17 (1976); (b) H. L. Tsai, J. Heising, J. L. Schindler, C. R. Kannewurf, and M. G. Kanatzidis, *Chem. Mater.* **9,** 879 (1997).
17. P. Joensen, R. F. Frindt, and S. R. Morrison, *Mater. Res. Bull.* **21,** 457 (1986).
18. G. Fu, L. F. Nazar, and A. D. Bain, *Chem. Mater.* **3,** 602 (1991).
19. Powder X-ray diffraction patterns were recorded using a Rigaku-Denki/RW400F2 (Rotaflex) rotating anode X-ray diffractometer using Cu$K\alpha$ radiation. Thermogravimetric measurements were obtained with a Shimadzu TG 50 instrument using oxygen or nitrogen flow and a heating rate of 5°C or 2°C/min. Conductivity measurements of the materials at room temperature were obtained for a pressed pellet using the four prong probe and a Keithley 236 source measure unit. Energy dispersive spectroscopy (EDS) was used to determine the ratios of Al to Mo on a JEOL-JSM-6400V at an accelerating voltage of 20 kV with samples mounted on nonaluminum stubs using carbon paint or carbon tape, equipped with a Tracor Northern 5500 X-ray microanalysis attachment. Solid state ^{27}Al MAS-NMR measurements were performed using a Varian 400MHz instrument tuned to 130.4 MHz pulse frequency, and at MAS frequencies of 4 and 6.2 MHz. BET surface area measurements were performed on a Quantasorb Jr. Sorption System using ultrapure nitrogen gas as the adsorbate and ultrapure helium gas as the carrier. The surface areas of the samples were calculated using the BET equation in Ref. (20).
20. S. Brunauer, P. H. Emmett, and Z. Teller, *J. Am. Chem. Soc.* **60,** 309 (1938).
21. J. Heising, H. L. Tsai, and M. G. Kanatzidis, unpublished results.
22. (a) Y. J. Liu, J. L. Schindler, D. C. DeGroot, C. R. Kannewurf, W. Hirpo, and M. G. Kanatzidis, *Chem. Mater.* **8,** 525 (1996); (b) Y. J. Liu, Ph.D. dissertation, Michigan State University, East Lansing, MI, 1994.
23. T. J. Pinnavaia, M. S. Tzou, S. D. Landau, and R. J. Raythatha, *J. Mol. Catal.* **27,** 195 (1984).
24. (a) Rietveld, *J. Appl. Crystallogr.* **2,** 65 (1969); (b) J. Rodriguez-Carvajal, "Abstracts of the Satellite Meeting on Powder Diffraction of the XVth Congress of the IUCr," p. 127, Toulouse, France, 1990.
25. The first two reflections were excluded from the refinement because their calculated intensities, whatever the structural model, were 2.7 and 1.7 times higher than the observed reflections. These huge discrepancies are mostly due to the deviation of the Lorentz factor from the ideal random powder case, tacitly employed in every Rietveld refinement software. In the case of a high, but not extreme, preferred orientation of the specimen, the relative intensities of the medium-to-high angle peaks are not much influenced by this effect. For details see: (a) R. C. Reynolds, *Clays and Clay Minerals* **34,** 359 (1986); (b) D. L. Bish and J. E. Post, Eds., "Modern Powder Diffraction, Reviews in Mineralogy," **20** Chapter 6. The Mineralogical Society of America, Washington DC, 1989; (c) G. M. Sheldrick, C. Kruger, and R. Goddard, Eds., "Crystallographic Computing 3: Data Collection, Structure Determination, Proteins, and Databases," p. 247. Clarendon Press, Oxford, 1985.
26. (a) R. A. Young and D. B. Wiles, *J. Appl. Crystallogr.* **15,** 430 (1982); (b) G. Cagliotti, A. Pelotti, and R. P. Ricci, *Nucl. Instrum. Methods* **35,** 223 (1958); (c) J. F. Berar and G. Baldinozzi, *J. Appl. Crystallogr.* **26,** 128 (1993).
27. Reasonable and fixed isotropic displacement parameters were assigned to the various atom types: $B_W = 1.5$ Å^2, $B_S = 2.0$ Å^2, $B_{Al} = 2.5$ Å^2, $B_O = 3.0$ Å^2, and only an overall temperature factor was refined. The $[Al_{13}O_{40}]$ cluster was treated as a rigid body, the z positional parameter of all the atoms in the cluster being constrained to follow the same shift. The population parameter was fixed at the value determined from EDS measurements. The position of the sulfur layer was also refined, giving a total of four free intensity-dependent parameters: $B_{overall}$, $z_{cluster}$, z_s, and the scale factor.
28. J. Durbin and G. S. Watson, *Biometrika* **58,** 1 (1971).
29. J. F. Berar and P. Lelann, *J. Appl. Crystallogr.* **24,** 1 (1991).
30. L. F. Nazar, S. W. Liblong, and X. T. Yin, *J. Am. Chem. Soc.* **113,** 5889 (1991).
31. Samples were converted to oxides by heating to 650°C under a stream of O_2. This was necessary because the X-ray emission lines (for EDS) of Mo and S overlap completely, hindering quantitative analysis.
32. The amount of water in the sample can be estimated if one assumes that when heated under oxygen, the aluminum cluster will decompose to form Al_2O_3, and MoS_2 will convert to MoO_3. Additional weight loss can be attributed to the water.
33. (a) D. Yang, J. J. Sandoval, W. M. R. Divigalpitiya, J. C. Irwin, R. F. Frindt, *Phys. Rev. B* **43,** 12053 (1991); (b) M. A. Py and R. R. Haering, *Can. J. Phys.* **61,** 76 (1983).
34. In order to probe the state of the Al cluster after the heating treatment (120°C for 18 h) required before the surface area measurements, we performed ^{27}Al solid state magic angle spinning NMR experiments. The spectrum clearly indicates that the structure of the intercalated species has been altered, possibly through oligomerization. This could result in blockage of any void space and could account for the observed low surface areas. Interestingly, the X-ray powder diffraction pattern does not change appreciably, so it cannot by itself be used as a structural diagnostic regarding the state of the aluminum cluster.